

MHD Radiative Boundary Layer Flow of a Nanofluid past a Stretching Sheet

Md. Shakhaoath Khan¹, Md. Mahmud Alam^{2,*} and M. Ferdows³

^{1,2} Mathematics Discipline, Khulna University, Khulna-9208, Bangladesh

*Email: alam_mahmud2000@yahoo.com

Email: shakhaoathmathku@yahoo.com

³ Departments of Mathematics, University of Dhaka, Dhaka-1000, Bangladesh

Email: ferdowsmohammad@yahoo.com

Abstract- The study of radiative heat transfer in a nanofluid within the influence of magnetic field over a stretching surface has been investigated numerically. This model is used for the laminar boundary layer flow of a nanofluid. Rosseland approximation is used to represent the radiative heat transfer. A similarity solution is presented here. The equation of momentum, energy and concentration are transformed into nonlinear ordinary coupled differential equations which depend on the Magnetic parameter M , Radiation parameter R , Prandtl number P_r , Eckert number E_c , Lewis number L_e , Brownian motion parameter N_b and Thermophoresis parameter N_t , respectively. These equations are solved numerically using the Nactsheim-Swigert shooting iteration technique together with Runge-Kutta six order iteration scheme. Numerical results are obtained for the temperature and concentration distributions, as well as local Nusselt number and local Sherwood number for several values of the corresponding parameters. The obtained results are presented graphically also in tabular form and the physical aspects of the problem are discussed.

Keywords: Nanofluid, Magnetic field, Thermal Radiation, Stretching Sheet

1. INTRODUCTION

The study of Magnetohydrodynamics (MHD) boundary layer flow of a nanofluid over a stretching surface has become the basic of several industrial, scientific and engineering applications. Engineers employ MHD principle in the design of heat exchangers, pumps and flow matters, in space vehicle propulsion, thermal protection, controlling the rate of cooling, controlling fusion etc. A number of technical processes concerning polymers involve the cooling of continuous strips or filaments by drawing them through a quiescent fluid. Further glass blowing, manufacture of plastic and rubber sheet, continuous casting of metals and spinning of flows involve the flow due to a stretching surface.

From the point of applications, several scientists have made model studies. Among them Carragher and Crane [1] investigated the heat transfer in the flow over a stretching surface in the case when the temperature difference between the surface and the ambient fluid is proportional to a power of distance from the fixed point. Na and Pop [2] studied an unsteady flow past a stretching sheet. M Alam *et al.* [3] showed the similarity solution for MHD flow through vertical porous plate with suction. Pop *et al.* [4] investigated the flow over stretching sheet near a stagnation point taking the effect of thermal radiation. Kumer [5] investigate the radiative heat transfer with the viscous dissipation effect in the presence transverse magnetic field. Singh *et al.* [6]

studied the effect of thermal radiation and magnetic field on unsteady stretching permeable sheet in presence of free stream velocity.

The research on nanofluids is gaining a lot of attention in recent years. Kang and Choi [7] studied the analysis of convective instability and heat transfer characteristics of the nanofluids. Jang and Choi [8] showed effect of various parameters on nanofluid thermal conductivity. Very recently, the convective heat transfers in a nanofluid past a vertical plate have studied by Kuznestov and Neild [9]. Khan and Pop [12] have studied the problem of laminar fluid flow over the stretching surface in a nanofluid and they investigated it numerically.

The objective of this study is to present a similarity analysis from the problem of steady boundary layer flow of a nanofluid past a stretching sheet with the influence of magnetic field and thermal radiation. The governing equations are transformed into nonlinear coupled ordinary differential equations which depend on the Magnetic parameter M , the Radiation parameter R , the Prandtl number P_r , the Eckert number E_c , the Lewis number L_e , the Brownian motion parameter N_b and the Thermophoresis parameter N_t . These equations are solved numerically using Nactsheim-Swigert [11] shooting iteration technique together with Runge-Kutta six order iteration schemes. The temperature and concentration distributions for the boundary layer flow of

*Corresponding author

a nanofluid are discussed and presented graphically. Also the surface heat transfer rate and mass transfer rate at the sheet are investigated.

2. PROBLEM FORMULATIONS

The steady two dimensional boundary layer flow of a nanofluid past a stretching surface is considered with the linear velocity $u_w = ax$, where a is a constant and x is a coordinate measured along the stretching surface. The flow model and coordinate system are shown in Fig.1.

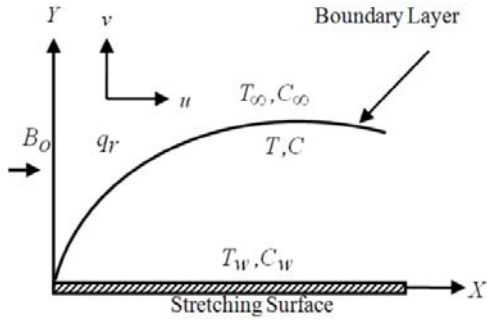


Fig.1: Physical configuration and coordinates system

The flow takes place at $y \geq 0$ where y is the coordinate measured normal to the stretching surface. A steady uniform stress leading to equal and opposite forces is applied along the x -axis, so that the sheet is stretched keeping the origin fixed. It is assumed that at the stretching surface, the temperature T , and the concentration C take constant value T_w and C_w respectively. The ambient values attained as y tends to infinity of T and C are denoted by T_∞ and C_∞ respectively.

A uniform magnetic field B_0 is imposed to the plate. The magnetic vector B_0 can be taken as $B = (0, B_0, 0)$.

And q_r is radiative heat flux in the y -direction. Consider the velocity components in x and y direction is u and v respectively. The velocity of the plate (uniform velocity) considered as U . Also a and b are the linear stretching constant, l is the characteristics length and A_1, A_2 is the constant whose values depends on the properties of the fluid.

Under the usual boundary layer approximation, the MHD flow and heat and mass transfer with the radiation effect are governed by the following equations;

The Continuity equation;

$$\frac{\partial u}{\partial x} + \frac{\partial v}{\partial y} = 0 \quad (1)$$

The Momentum equation;

$$u \frac{\partial u}{\partial x} + v \frac{\partial u}{\partial y} = U \frac{dU}{dx} + \nu \frac{\partial^2 u}{\partial y^2} + \frac{\sigma B_0^2}{\rho} (U - u) \quad (2)$$

The Energy equation;

$$u \frac{\partial T}{\partial x} + v \frac{\partial T}{\partial y} = \alpha \frac{\partial^2 T}{\partial y^2} - \frac{\alpha}{k} \frac{\partial q_r}{\partial y} + \frac{\nu}{c_p} \left(\frac{\partial u}{\partial y} \right)^2 + \tau \left\{ D_B \left(\frac{\partial T}{\partial y} \cdot \frac{\partial C}{\partial y} \right) + \frac{D_T}{T_\infty} \left(\frac{\partial T}{\partial y} \right)^2 \right\} \quad (3)$$

The Concentration equation;

$$u \frac{\partial C}{\partial x} + v \frac{\partial C}{\partial y} = D_B \frac{\partial^2 C}{\partial y^2} + \frac{D_T}{T_\infty} \frac{\partial^2 T}{\partial y^2} \quad (4)$$

And the boundary condition for the model is;

$$u = u_w = ax, v = 0, T = T_w = T_\infty + A_1 \left(\frac{x}{l} \right)^m,$$

$$C = C_w = C_\infty + A_2 \left(\frac{x}{l} \right)^m \quad \text{at } y = 0$$

$$u = U = bx, T \rightarrow T_\infty, C \rightarrow C_\infty \quad \text{as } y \rightarrow \infty \quad (5)$$

where, x is the coordinate measured along stretching surface, u_w is the stretching velocity, U is the uniform velocity, a and b are the linear stretching constant, l is the characteristics length and A_1, A_2 is the constant whose values depends on the properties of the fluid.

Rosseland approximation [10] has been considered for radiative heat flux and leads to the form as,

$$q_r = - \frac{4\sigma}{3\kappa^*} \frac{\partial T^4}{\partial y} \quad (6)$$

where, σ is the Stefan-Boltzmann constant and κ^* is the mean absorption coefficient.

In order to attain a similarity solution to Eqs. (1) to (4) with the boundary conditions (5) the following dimensionless variables are used,

$$\eta = y \sqrt{\frac{a}{\nu}}, \psi = x \sqrt{a\nu} f(\eta), \theta = \theta(\eta) = \frac{T - T_\infty}{T_w - T_\infty},$$

$$\phi = \phi(\eta) = \frac{C - C_\infty}{C_w - C_\infty}, u = \frac{\partial \psi}{\partial y}, v = - \frac{\partial \psi}{\partial x} \quad (7)$$

From the above transformations the non dimensional, nonlinear, coupled ordinary differential equations are obtained as;

$$f''' + ff'' - f'^2 + M \left(\frac{b}{a} - f' \right) + \frac{b^2}{a^2} = 0 \quad (8)$$

$$(1+R)\theta'' + E_c P_r f'^{1/2} + P_r f\theta' - m P_r f'\theta + P_r N_b \theta'\phi' + P_r N_t \theta'^2 = 0 \quad (9)$$

$$\phi'' + L_e f\phi' + \frac{N_t}{N_b} \theta'' - L_e m f'\phi = 0 \quad (10)$$

and the corresponding boundary conditions,

$$\left. \begin{aligned} f = 0, f' = 1, \theta = 1, \phi = 1, \text{ at } \eta = 0 \\ f' = \frac{b}{a}, \theta = 0, \phi = 0, \text{ as } \eta \rightarrow \infty \end{aligned} \right\} \quad (11)$$

where the notation primes denote differentiation with respect to η and the seven parameters are defined by

$$M = \frac{\sigma B_0^2}{\rho a}, R = \frac{16\sigma T_\infty^3}{3k\kappa^*}, p_r = \frac{\nu}{\alpha}, L_e = \frac{\nu}{D_B},$$

$$E_c = \frac{u_w^2}{c_p(T_w - T_\infty)}, N_b = \frac{(\rho c)_p D_B (\phi_w - \phi_\infty)}{\nu(\rho c)_f},$$

$$N_t = \frac{(\rho c)_p D_T (T_w - T_\infty)}{\nu T_\infty (\rho c)_f} \quad (12)$$

where $M, R, P_r, E_c, L_e, N_b, N_t$ and $\frac{b}{a}$ denote the Magnetic parameter, the Radiation parameter, the Prandtl number, the Eckert number, the Lewis number, the Brownian motion parameter, the Thermophoresis parameter and the stretching parameter respectively.

The physical quantities of the reduced Nusselt number and reduced Sherwood number are calculated respectively by the following equations,

$$N_u (R_e)^{\frac{1}{2}} = -\theta'(0), \quad S_h (R_e)^{\frac{1}{2}} = -\phi'(0).$$

Where, $R_e = \frac{xu_w(x)}{\nu}$ is the Reynolds number.

3. NUMERICAL PROCEDURE

Eqs. (8) to (10) with boundary condition (11) are solved numerically using standard initially value solver the shooting method. For the purpose of this method, the Nactsheim-Swigert shooting iteration technique [11] together with Runge-Kutta six order iteration scheme is taken and determines the temperature and concentration as a function of the coordinate η . Extension of the iteration shell to above equation system of differential equations (11) is straightforward, there are three asymptotic boundary condition and hence three unknown surface conditions $f''(0), \theta'(0)$ and $\phi'(0)$.

4. RESULTS AND DISCUSSION

For the accuracy of the numerical results the present results are compared with the solution of Khan and Pop [12] and the values of Magnetic parameter M , Radiation parameter R , Eckert number E_c , Stretching parameter $\frac{b}{a}$ and constant parameter m are considered zero. Also the effects of above parameters are shown in the present study. The results for the reduced Nusselt number are compared in Table 1.

Table 1: Comparison of results for the reduced Nusselt number when $P_r = L_e = 10, M = 0, R = 0, E_c = 0, \frac{b}{a} = 0$ and $m = 0$.

$N_b = N_t =$	Present Results	Khan and Pop [12]
0.1	0.9524	0.9524
0.2	0.3653	0.3654
0.3	0.1351	0.1355
0.4	0.0490	0.0495
0.5	0.0178	0.0179

The graphical representation of the problem has been showed in Comparison Figs. 3, 5, 7, 9 and Figs. 10-13. And these results (Comparison Figs. 3, 5, 7, 9) have been compared with the published results of Khan and Pop [12] (see Comparison Figs. 2, 4, 6 and 8 respectively).

Comparison Fig. 2 shows the effects of Brownian motion parameter N_b and thermophoresis parameter N_t on the temperature profile for several parameters as

Prandtl number $P_r = 10$, Lewis number $L_e = 10$. For comparison, the values of radiation parameter R , magnetic parameter M , Eckert number E_c , stretching parameter $\frac{b}{a}$ and constant parameter m are considered zero as well as $R = 1, M = 1, E_c = .01, \frac{b}{a} = 2.5$ and $m = 1$.

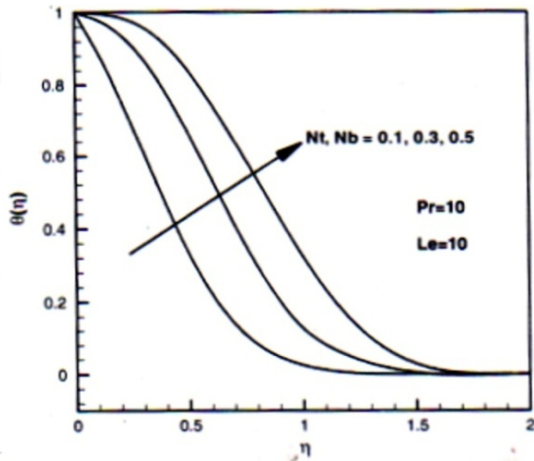
And the result has shown in comparison Fig. 3. For the above cases the results shows temperature increases as the thermophoresis parameter N_t and the Brownian motion parameter N_b increases. Therefore the qualitative agreement has been seen in these two figures and the agreement is good.

Comparison Fig. 4 represents the concentration distribution for the different values of Brownian motion parameter N_b and specified parameters as Prandtl number $P_r = 10$, Lewis number $L_e = 10$, thermophoresis parameter $N_t = 0.1$. For comparison, the values of radiation parameter R , magnetic parameter M , Eckert number E_c , Stretching parameter $\frac{b}{a}$ and constant parameter m are considered zero as well as

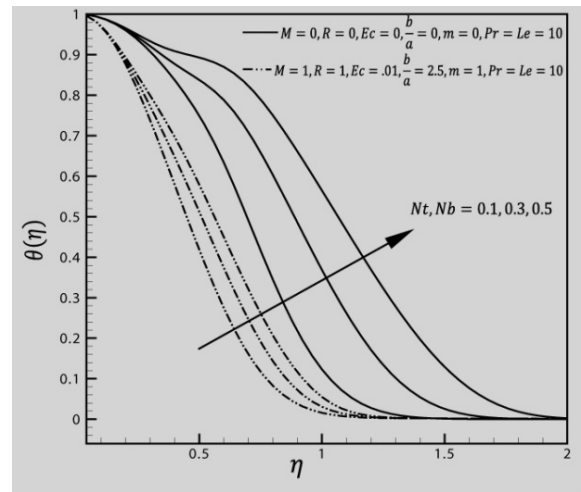
$R = 1, M = 1, E_c = .01, \frac{b}{a} = 2.5$ and $m = 1$. And the result has shown in comparison Fig. 5. It is observed that the thickness of the boundary layer for the mass fraction function is to be smaller than the thermal boundary layer thickness when $L_e > 1$. For the above cases, concentration profiles are decreases with increase in Brownian motion parameter N_b and when $N_b > 0.5$, this decrease diminishes. Therefore the qualitative agreement has been seen in these two figures and the agreement is good.

Comparison Fig. 6 represents the effects of Prandtl number P_r and Lewis number L_e on the temperature distribution for several values as Brownian motion parameter $N_b = 0.5$ and thermophoresis parameter $N_t = 0.5$. For comparison, the values of radiation parameter R , magnetic parameter M , Eckert number E_c , Stretching parameter $\frac{b}{a}$ and constant parameter m are considered zero as well as $R = 1, M = 1, E_c = .01, \frac{b}{a} = 2.5$ and $m = 1$. And the result has shown in comparison Fig. 7. The same results have found for the above cases as the temperature decreases with the increase in both Prandtl number P_r and Lewis number L_e . Therefore the qualitative agreement has been seen in these two figures and the agreement is good.

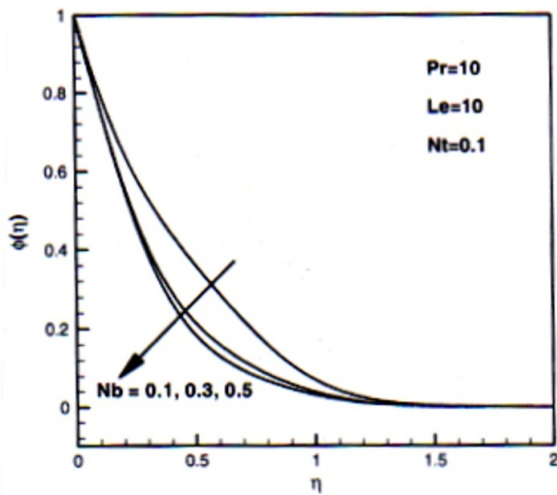
Comparison Fig. 8 represents the effects of Lewis number L_e on the concentration profiles for Prandtl number $P_r = 10$, thermophoresis parameter $N_t = 0.1$, and Brownian motion parameter $N_b = 0.1$. For comparison, the values of radiation parameter R , magnetic parameter M , Eckert number E_c , Stretching parameter $\frac{b}{a}$ and constant parameter m are considered zero as well as $R = 1, M = 1, E_c = .01, \frac{b}{a} = 2.5$ and $m = 1$. And the result has shown in comparison Fig. 9. It is observed that, if the Lewis number L_e increases, the concentration profiles decreases gradually. Therefore the qualitative agreement has been seen in these two figures and the agreement is good.



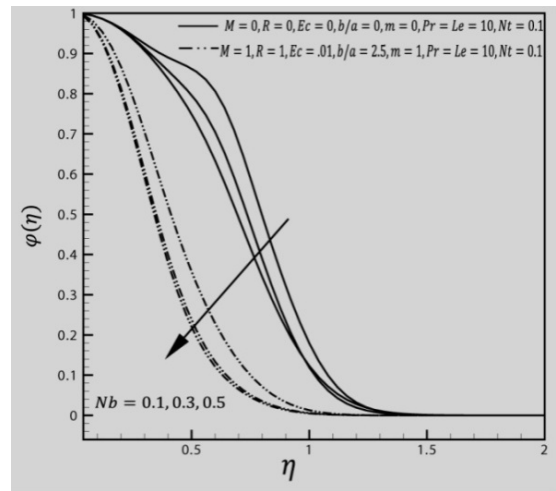
Comparison Fig.2: Effect of N_b and N_t on temperature profiles



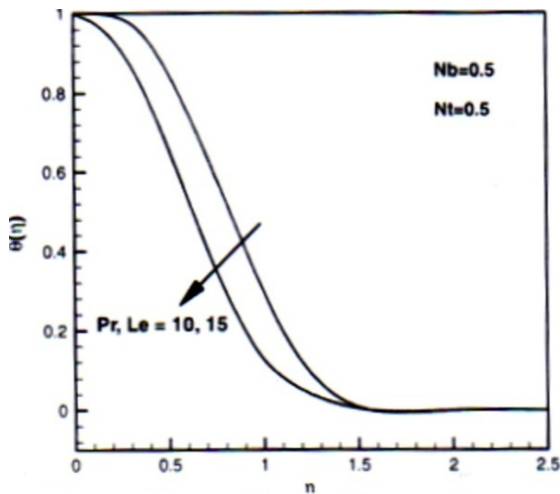
Comparison Fig.3: Effect of N_b and N_t on temperature profiles



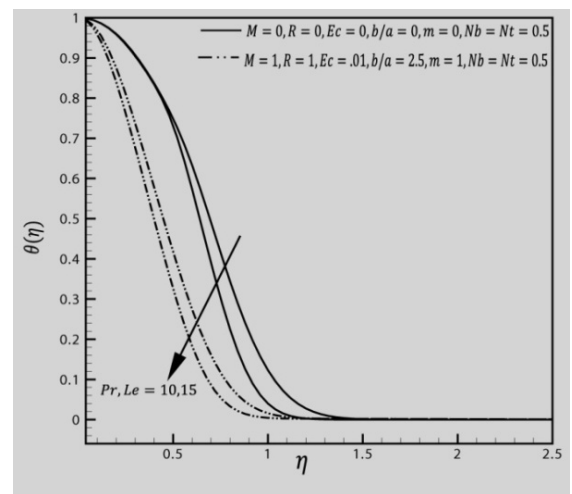
Comparison Fig.4: Effect of N_b on concentration profiles



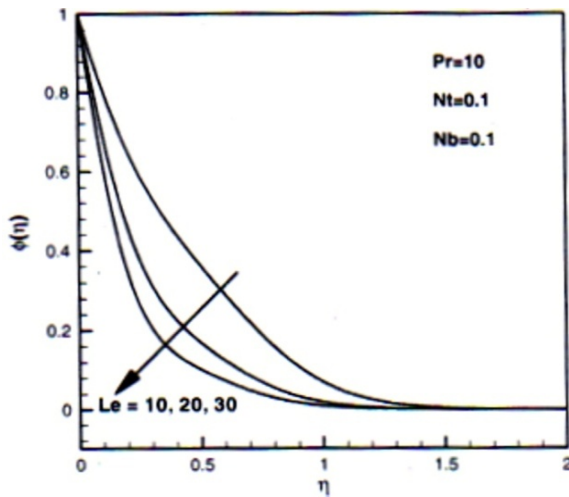
Comparison Fig.5: Effect of N_b on concentration profiles



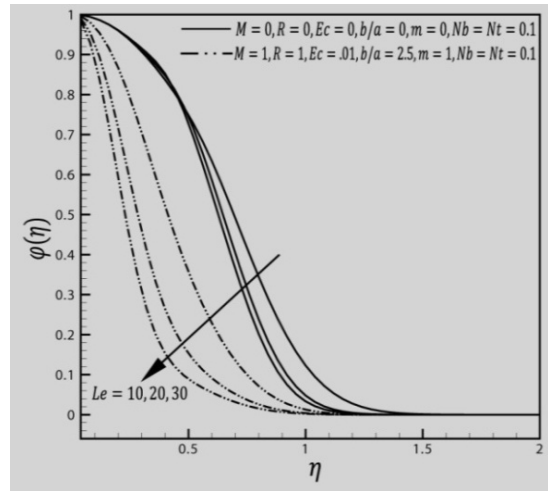
Comparison Fig.6: Effect of P_r and L_e on temperature profiles



Comparison Fig.7: Effect of P_r and L_e on temperature profiles



Comparison Fig.8: Effect of L_e on concentration profiles



Comparison Fig.9: Effect of L_e on concentration profiles

Since the physical interest of the problem, the dimensionless heat transfer rates plotted against N_t and shown in Figs. 10 and 12. This variation shows the effects of N_b on the dimensionless heat transfer rates at the sheet for different L_e . It may conclude that the dimensionless heat transfer rate at the sheet decreases for increasing N_b .

Figs. 11 and 13 shows the dimensionless concentration

rates plotted against N_t for the corresponding parameters and for different L_e . In Fig. 11, dimensionless concentration rates at the sheet decreases with increase in N_b . Fig. 13 shows the same effects with the corresponding parameters. The increase in dimensionless mass transfer rates is monotonic for large Lewis number.

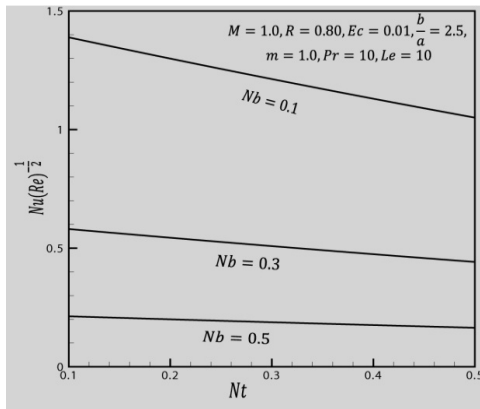


Fig.10: Effect of N_b on dimensionless heat transfer rates

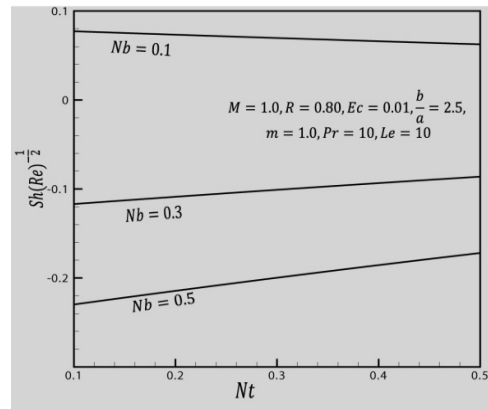


Fig.11: Effect of N_b on dimensionless concentration rates

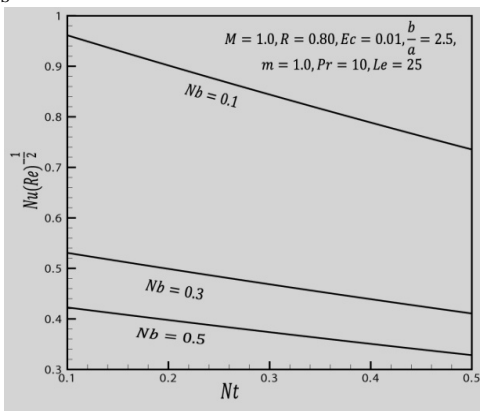


Fig.12: Effect of N_b on dimensionless heat transfer rates

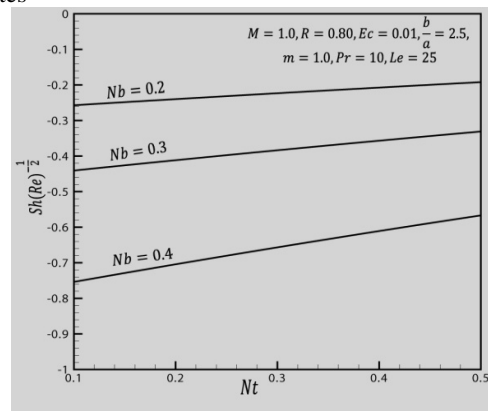


Fig.13: Effect of N_b on dimensionless concentration rates

5. CONCLUSIONS

Laminar boundary layer flow of a nanofluid has been investigated for steady flow over the stretching surface with the influence of magnetic field and thermal radiation. The temperature and concentration effects and heat and mass transfer rates at the sheet for corresponding parameters are studied and shown graphically. A considerable comparison with Khan and Pop [12] has been showed and the comparison shows a good agreement. Also the effect of magnetic field and thermal radiation are showed on temperature and concentration profiles for the flow past a stretching sheet.

6. REFERENCES

- [1] P. Carragher, L. Crane, "Heat Transfer on Continuous Stretching Sheet", *Journal of Applied mathematics and Mechanics*, vol. 62, no. 10, pp. 564-565, 1982.
- [2] T. Y. Na and I. Pop, "Unsteady flow past a stretching sheet", *Mechanical Research Communications*, vol. 23, pp. 413-422, 1996.
- [3] M. Ferdows, Ota, Sattar and M. M. Alam, "Similarity Solution for MHD Flow through a Vertical Porous Plate with Suction", *Journal of Computational and Applied Mechanics*, vol. 6, no.1, pp. 15-25, 2005.
- [4] S. R. Pop, T. Grosan and I. Pop., "Radiation effect on the flow near the stagnation point of a stretching sheet", *Technische Mechanik*, vol. 25, pp. 100-106, 2004.
- [5] H. Kumar, "Radiative Heat Transfer with Hydro magnetic flow and Viscous Dissipation over a Stretching surface in the Presence of Variable Heat Flux", *Thermal Science*, vol. 13, no. 2, pp.163-169, 2009.
- [6] P. Singh, Jangid, N.S. Tomer, and D. Sinha, "Effects of Thermal Radiation and Magnetic Field on Unsteady Stretching Permeable Sheet in Presence of Free Stream Velocity", *International Journal of Information and Mathematical Science*, vol. 6, no. 3, 2010.
- [7] K. I. Kang, J. Y. T. and C. K. Choi, "Analysis of Convective Instability and Heat Transfer Characteristics of Nanofluids", *Physics of Fluids*, vol. 16, no. 7, pp. 2395-2401, 2004.
- [8] S. P. Jang, and S. U. S. Choi, "Effects of Various Parameters on Nanofluid Thermal Conductivity", *Journal of Heat Transfer*, vol. 129, pp. 617-623, 2007.
- [9] A. V. Kuznetsov, and D.A. Nield, "Natural Convective Boundary- layer Flow of a Nanofluid Past a Vertical Plate", *International Journal of Thermal Sciences*, vol. 49, pp. 243-247, 2010.
- [10] M. Q. Brewster, *Thermal Radiative Transfer and Properties*, John Wiley and Sons Inc: New York, USA, 1992.
- [11] P. R. Nachtsheim, and P. Swigert, "Satisfaction of the asymptotic boundary conditions in numerical solution of the system of non-linear equations of boundary layer type", NASA TND-3004, 1995.

- [12] W. A. Khan, and I. Pop, "Boundary-Layer Flow of a Nanofluid Past a Stretching Sheet", *International Journal of Heat and Mass Transfer*, vol. 53, pp. 2477-2483, 2010.

7. NOMENCLATURE

a & b	linear stretching constants
A_1, A_2	constants depends on the properties of the fluid
l	characteristics length
C	nanoparticle concentration
C_w	nanoparticle concentration at stretching surface
C_∞	ambient nanoparticle concentration
T	fluid temperature
T_w	temperature at the stretching surface
T_∞	ambient temperature
B_0	magnetic induction
k	thermal conductivity
κ	Boltzmann constant, $1.3805 \times 10^{-23} \text{ J / K}$
c_p	specific heat capacity
p	fluid pressure
D_B	Brownian diffusion coefficient
D_T	thermophoresis diffusion coefficient
u_w	stretching velocity
κ^*	mean absorption coefficient
q_r	radiative heat flux in the y-direction
U	uniform velocity
x, y	Cartesian coordinates (y is normal to x axis)
u, v	velocity components (along x and y respectively)

Parameters

p_r	Prandtl number
L_e	Lewis number
N_b	Brownian motion parameter
N_t	Thermophoresis parameter
M	Magnetic parameter
E_c	Eckert number
R	Radiation parameter
N_u	Nusselt Number
S_h	Sherwood number

Greek Symbols

ν	kinematic viscosity of the fluid
μ	dynamic viscosity
$(\rho c)_p$	effective heat capacity of the nanoparticle material
$(\rho c)_f$	effective heat capacity of the fluid
α	thermal diffusivity
σ_s	Stefan-Boltzmann constant, $5.6697 \times 10^{-8} \text{ W / m}^2 \text{ K}^4$
σ	conductivity of the material
η	similarity variable
ψ	stream function
$\theta(\eta)$	dimensionless temperature
$\phi(\eta)$	Dimensionless concentration
ρ_p	nanoparticle mass density
ρ_f	fluid density
τ	ratio between the effective heat capacity of the nanoparticle material and heat capacity of the fluid